Hyperfine-induced modifications to the angular distribution of the $K\alpha_1$ x-ray emission

Z. W. Wu,[1,2] A. Surzhykov,[1] and S. Fritzsche[1,3]
[1]*Helmholtz-Institut Jena, D-07743 Jena, Germany*
[2]*Key Laboratory of Atomic and Molecular Physics & Functional Materials of Gansu Province, College of Physics and Electronic Engineering, Northwest Normal University, Lanzhou 730070, People's Republic of China*
[3]*Theoretisch-Physikalisches Institut, Friedrich-Schiller-Universität Jena, D-07743 Jena, Germany*
(Received 20 January 2014; published 19 February 2014)

The angular distribution of the $K\alpha_1$ ($1s2p_{3/2}\ ^{1,3}P_{1,2} \rightarrow 1s^2\ ^1S_0$) x-ray emission following the radiative electron capture into initially hydrogenlike ions with nonzero nuclear spin has been studied within the density matrix theory and the multiconfiguration Dirac-Fock method. Emphasis is placed especially upon the hyperfine interaction and how this interaction of the magnetic moment of the nucleus with those of the electrons affects the angular properties of the $K\alpha_1$ radiation. Calculations were performed for selected isotopes of heliumlike Sn^{48+}, Xe^{52+}, and Tl^{79+} ions. A quite sizable contribution of the hyperfine interaction upon the $K\alpha_1$ angular emission is found for isotopes with nuclear spin $I = 1/2$, while its effect is suppressed for (most) isotopes with nuclear spin $I > 1/2$. We therefore suggest that accurate measurements of the $K\alpha_1$ angular distribution at ion storage rings can be utilized as a tool for determining the nuclear parameters of rare stable and radioactive isotopes with $I \geqslant 1/2$.

DOI: 10.1103/PhysRevA.89.022513 PACS number(s): 31.10.+z, 31.15.aj

I. INTRODUCTION

In recent decades, the angular distribution of the characteristic x-ray emission of highly charged ions has been investigated, both theoretically [1,2] and experimentally [3–5]. When compared to measurements of the total decay rates of these ions, such angle-resolved studies were found to be much more sensitive to the details of the various effects and interactions and, in fact, helped provide new insight into the electron-electron [6–8] and electron-photon [9–11] interactions in the presence of strong Coulomb fields.

Detailed measurements of the characteristic x rays of highly charged ions have been carried out especially at the GSI experimental storage ring (ESR) in Darmstadt following the radiative electron capture (REC) into initially either bare or hydrogenlike ions. While, for example, the observed Lyman-α_1 radiation following the electron capture into the $2p_{3/2}$ state of (finally) hydrogenlike ions displayed a strong anisotropic angular pattern [12], the $K\alpha_1$ emission from the decay of heliumlike $1s2p_{3/2}$ states was found to be almost isotropic [13]. However, such a qualitative difference between the Lyman-α_1 and $K\alpha_1$ emission patterns can be understood quite easily if the $1s2p_{3/2}\ ^{1,3}P_{1,2} \rightarrow 1s^2\ ^1S_0$ fine structure of the $K\alpha_1$ radiation is taken into consideration. The small anisotropy of the $K\alpha_1$ radiation is caused then by the opposite (angular) behavior of the $1s2p_{3/2}\ ^1P_1 \rightarrow 1s^2\ ^1S_0$ electric-dipole (E1) and $1s2p_{3/2}\ ^3P_2 \rightarrow 1s^2\ ^1S_0$ magnetic-quadrupole (M2) fine-structure components to the overall $K\alpha_1$ line [14,15]. From a detailed analysis of this mutual cancellation of the E1 and M2 decay channels to the $K\alpha_1$ angular distributions, valuable knowledge could be revealed about the structure and dynamics of heliumlike ions. In addition, further information about the electron-electron and electron-photon interactions in strong Coulomb fields was obtained also from recent polarization measurements of the Lyman-α_1 and $K\alpha_1$ radiations [16].

Until now, however, most experimental and theoretical studies on the characteristic x-ray emission have just dealt with heavy ions having zero nuclear spin, $I = 0$, or have simply omitted all contributions that arise from such a spin. Little attention has been paid so far to the effect of the hyperfine interaction for isotopes with $I \neq 0$, and how the nuclear spin may affect the characteristic x-ray emission. Early work on the angular and polarization properties of the characteristic x rays from ions with $I \neq 0$ was performed by Dubau and co-workers [17–19] and, more recently, also by us [20]. In these investigations, the hyperfine-induced effects were studied for the decay of heliumlike ions following either the electron-impact excitation or the REC into the $1s2p\ ^3P_2$ and $^1P_1$ levels, respectively. Hereby, the main emphasis was just placed on the individual hyperfine- or fine-structure-resolved transitions whose properties were found to be strongly affected by the magnetic dipole moment μ_I of the nucleus. In the high-Z domain, however, the observation of individual fine- or even hyperfine-resolved transitions is very unlikely due to the small hyperfine splitting as well as the restricted energy resolution of modern x-ray detectors. It is therefore important to analyze and better understand how the hyperfine interaction affects the properties of the overall $K\alpha_1$ line as obtained from the (yet) unresolved hyperfine- and fine-structure components.

In the present work, we investigate the $K\alpha_1$ x-ray emission following the REC into the excited $1s2p_{3/2}\ ^{1,3}P_{1,2}$ levels of (finally) heliumlike ions with *nonzero* nuclear spin. Emphasis is placed upon the question of how the hyperfine interaction affects the (hyperfine- and fine-structure *averaged*) angular properties of the $K\alpha_1$ radiation for isotopes with $I \neq 0$. A rather strong influence of the hyperfine interaction upon the $K\alpha_1$ line is found, especially for isotopes with nuclear spin $I = 1/2$ (and with typical nuclear magnetic moments μ_I of either sign), while these effects are less important for isotopes with nuclear spin $I > 1/2$. We therefore suggest that (accurate) measurements of the $K\alpha_1$ angular distribution can be utilized as an independent tool for studying the nuclear parameters of rare stable or radioactive isotopes at ion storage rings.

In the next section, we first outline the theoretical description of the angle-resolved photon emission from medium- and high-Z ions. We continue here our previous work on

the linear polarization of the hyperfine-resolved $K\alpha_1$ emission for heliumlike ions [20] and explain how an *effective* anisotropy parameter can be defined for isotopes with nonzero nuclear spin, and without any need to resolve the individual hyperfine- and fine-structure transitions explicitly. The effective anisotropy parameters and angular distribution, calculated for selected heliumlike isotopes with different nuclear spins and magnetic dipole moments, are then presented in Sec. III. Finally, brief conclusions of the present work are given in Sec. IV.

II. THEORETICAL BACKGROUND

Let us start with considering the following two-step process:

$$A^{(Z-1)+}(1s) + e^- \longrightarrow A^{(Z-2)+}\left(1s2p_{3/2}\ ^{1,3}P_{1,2}\right) \longrightarrow A^{(Z-2)+}\left(1s^2\ ^1S_0\right) + K\alpha_1, \quad (1)$$

in which an initially hydrogenlike ion $A^{(Z-1)+}$ in its ground state and with nuclear charge Z captures a free (or quasifree) electron and forms one of the excited $1s2p_{3/2}\ ^{1,3}P_{1,2}$ fine-structure levels of the (finally) heliumlike ion, $A^{(Z-2)+}$. The subsequent radiative decay of these excited levels then gives rise to what is known as the $K\alpha_1$ emission, which is typically observed without resolving the associated fine or hyperfine transitions. Indeed, the formation of the excited $1s2p_{3/2}\ ^{1,3}P_{1,2}$ levels can be described independently from the subsequent photon emission and without the need to incorporate the hyperfine interaction into the capture process, i.e., the first step in the process (1), as long as the initial ions and electrons are not polarized themselves.

A. Alignment of excited ions

Often, the process (1) is observed at ion storage rings, and then the (ion) beam *naturally defines* the direction with regard to which the excited heliumlike ions will be (more or less) aligned, in dependence of the energy of the projectiles or due to further details in the prior electron excitation or capture process [12,16]. This alignment of the ions, i.e., their nonequal population of the magnetic sublevels with different modulus of the magnetic quantum number $|M_{J_i}|$, is usually described in terms of so-called alignment parameters $\mathcal{A}_{k0}(\alpha_i J_i)$. These parameters completely characterize the formation process and, hence, enable one to just describe the subsequent photon emission without further reference to the details of the excitation process.

The formation of the excited $1s2p_{3/2}\ ^{1,3}P_{1,2}$ levels of heliumlike ions following the REC into initially hydrogenlike ions has been explored in great detail in Refs. [14,21] by applying the density matrix theory. Therefore, we shall recall here only the relevant formulas as needed to obtain the alignment and associated *effective* anisotropy parameters for ions with nonzero nuclear spin. Within the density matrix theory [22,23], the alignment parameter $\mathcal{A}_{k0}(\alpha_i J_i)$ of some ionic level $|\alpha_i J_i\rangle$ is related directly to the partial cross sections $\sigma_{|\alpha_i J_i M_i\rangle}$ for populating the different magnetic sublevels $|\alpha_i J_i M_i\rangle$. For the REC into the excited $1s2p_{3/2}\ ^{1,3}P_{1,2}$ levels, for example, these alignment parameters can be written in the form [21]

$$\mathcal{A}_{20}(^1P_1) = \sqrt{2}\,\frac{\sigma_{|1,\pm1\rangle} - \sigma_{|1,0\rangle}}{2\sigma_{|1,\pm1\rangle} + \sigma_{|1,0\rangle}}, \quad (2)$$

$$\mathcal{A}_{20}(^3P_2) = -\sqrt{\frac{10}{7}}\,\frac{\sigma_{|2,0\rangle} + \sigma_{|2,\pm1\rangle} - 2\sigma_{|2,\pm2\rangle}}{\sigma_{|2,0\rangle} + 2\sigma_{|2,\pm1\rangle} + 2\sigma_{|2,\pm2\rangle}}, \quad (3)$$

where $\sigma_{|1,0\rangle}$ and $\sigma_{|1,\pm1\rangle}$ refer to the partial REC cross sections for populating the $M = 0$ and $M = \pm1$ sublevels of the excited $^1P_1$ level and, similarly, $\sigma_{|2,0\rangle}$, $\sigma_{|2,\pm1\rangle}$, and $\sigma_{|2,\pm2\rangle}$ to the corresponding partial cross sections for sublevels of the excited $^3P_2$ level of heliumlike ions. Apart from the parameter $\mathcal{A}_{20}(^3P_2)$, the alignment of the $^3P_2$ level should be described also by a fourth-rank parameter $\mathcal{A}_{40}(^3P_2)$. For the REC into high-Z projectiles, however, this parameter $\mathcal{A}_{40}(^3P_2)$ is typically much smaller than the corresponding second-rank parameter $\mathcal{A}_{20}(^3P_2)$ [14,21], and can thus be neglected in the following analysis of the angular properties of the characteristic $K\alpha_1$ emission.

For isotopes with nonzero nuclear spin, $I \neq 0$, the fine-structure levels $|\alpha_i J_i\rangle$ will further split into (so-called) hyperfine levels $|\beta_i F_i\rangle$ with $\beta_i \equiv \alpha_i J_i I$ owing to the hyperfine interaction of the nuclear magnetic moment with those from the orbital and spin motion of the electrons. If the hyperfine interaction is incorporated only via the $I - J$ coupling but otherwise does not affect the excitation process, the alignment parameters $\mathcal{A}_{k0}(\beta_i F_i)$ of these hyperfine levels can be obtained from the alignment of the corresponding fine-structure level $|\alpha_i J_i\rangle$ by [20,24]

$$\mathcal{A}_{k0}(\beta_i F_i) = (-1)^{J_i+I+F_i-k}\,[J_i, F_i]^{1/2} \times \begin{Bmatrix} F_i & F_i & k \\ J_i & J_i & I \end{Bmatrix} \mathcal{A}_{k0}(\alpha_i J_i), \quad (4)$$

where $[a,b,\ldots] \equiv (2a+1)(2b+1)\cdots$ and the standard notation is used for the Wigner 6-j symbols. For initially unpolarized electrons and ions, these alignment parameters fully describe the magnetic sublevel population of the excited ions and, thus, can be utilized in order to express the angular and polarization properties of the subsequent photon emission.

B. Radiative decay of excited ions

To analyze the angular properties of the characteristic radiation, let us begin with the individual hyperfine-resolved transition $|\beta_i F_i\rangle \to |\beta_f F_f\rangle + h\nu$, for which the angular distribution reads [20]

$$W_{if}(\theta) = \frac{1}{4\pi}[1 + \mathcal{A}_{20}(\beta_i F_i)\ f_2(\beta_i F_i, \beta_f F_f) P_2(\cos\theta)]. \quad (5)$$

Here, $P_2(\cos\theta)$ denotes the second-order Legendre polynomial, θ the polar angle of the emitted photon with regard to the quantization (beam) axis, and $f_2(\beta_i F_i, \beta_f F_f)$ the so-called structure function which only depends on the electronic structure of the ions but is independent of the REC process; cf. Refs. [20–23] for further details.

Typically, however, neither the hyperfine- nor the fine-structure transitions can be resolved experimentally in the x-ray emission from high-Z ions. Therefore, in order to allow comparison with the measurements, we then need to

average over the angular distribution (5) to account for the contribution of the individual hyperfine transitions to the observed x-ray spectra. For the two $1s2p_{3/2}\ ^1P_1 \to 1s^2\ ^1S_0$ and $1s2p_{3/2}\ ^3P_2 \to 1s^2\ ^1S_0$ fine-structure components of the $K\alpha_1$ line, the angular distribution then reads [20]

$$W_{J=1,2}(\theta) = \frac{\sum_{F_i F_f} N_{if} W_{if}(\theta)}{\sum_{F_i F_f} N_{if}}, \tag{6}$$

where the summations over the total angular momentum quantum numbers, F_k, take the values $F_k = |I - J_k|, \ldots, I + J_k$, and where the N_{if} refer to proper weights for the contribution of the (individual) hyperfine components to the $|\alpha_i J_i\rangle \to |\alpha_f J_f\rangle$ fine-structure transition. For sufficiently short lifetimes of the excited levels, just in order to ensure that all or an equal portion of the emitted photons are indeed recorded at the detectors, these weights N_{if} are simply given by the relative population of the upper levels $|\beta_i F_i\rangle$ and, hence, by the partial cross sections for populating the excited sublevels [20]. In the following, we assume that the fine and hyperfine levels are populated only by the REC and just define $N_{if} = \sigma(\beta_i F_i)/\sum_{F_i} \sigma(\beta_i F_i)$, where $\sigma(\beta_i F_i)$ denotes the known REC cross sections [21].

Following similar routes, the angular distribution of the overall $K\alpha_1$ emission can be given by averaging, in addition, over its two fine-structure components $1s2p_{3/2}\ ^1P_1 \to 1s^2\ ^1S_0$ and $1s2p_{3/2}\ ^3P_2 \to 1s^2\ ^1S_0$,

$$W_{K\alpha_1}(\theta) = N_{J=1} W_{J=1}(\theta) + N_{J=2} W_{J=2}(\theta), \tag{7}$$

and with weights as obtained from the corresponding total cross sections for populating the upper levels, and if their branching ratios for a direct decay to the $1s^2\ ^1S_0$ ground state are taken into account. Alternatively, this angular distribution of the $K\alpha_1$ line can also be expressed by means of a single *effective* anisotropy parameter,

$$W_{K\alpha_1}(\theta) = \frac{1}{4\pi}\left[1 + \beta_2^{\rm eff}(K\alpha_1)\, P_2(\cos\theta)\right], \tag{8}$$

i.e., without the need (or any reference) to resolve the individual hyperfine- and fine-structure transitions.

Equations (5)–(8) are general and, thus, can be utilized in order to express the effective anisotropy parameter $\beta_2^{\rm eff}$ for the $K\alpha_1$ emission from heliumlike ions with either zero or nonzero nuclear spin. By inserting Eqs. (5) and (6) into Eq. (7), and by making use of Eq. (4) for the hyperfine-resolved transitions, this effective anisotropy parameter can be expressed in terms of the anisotropy parameters of the fine-structure transitions. For isotopes with nuclear spin $I = 1/2$, for example, the effective parameter becomes

$$\begin{aligned}\beta_2^{\rm eff}(K\alpha_1; I = 1/2) &= \frac{1}{3\sqrt{2}} N_{J=1} \mathcal{A}_{20}(^1P_1) + \frac{2}{5}\sqrt{\frac{7}{5}} N_{J=2} \mathcal{A}_{20}(^3P_2) \\ &\times \left(\frac{\sqrt{6}}{2}\frac{a_{\rm E1}}{a_{\rm M2}} - \frac{\sqrt{2}}{4} - \frac{3\sqrt{2}}{7}\right).\end{aligned} \tag{9}$$

In this formula, we have applied here the shorthand notation $a_{pL} = \langle 1s^2\ ^1S_0, F_f = 1/2 \| H_\gamma(pL) \| 1s2p_{3/2}\ ^3P_2, F_i = 3/2\rangle$ in order to denote the reduced amplitudes for the leading M2 and hyperfine-induced E1 components of the $1s2p_{3/2}\ ^3P_2, F_i = 3/2 \to 1s^2\ ^1S_0, F_f = 1/2$ fine-structure transition; cf. the red line in Fig. 1. In some more detail, these amplitudes arise from the structure functions of the associated hyperfine-resolved transitions. For the $1s2p_{3/2}\ ^1P_1, F_i = 3/2 \to 1s^2\ ^1S_0, F_f = 1/2$ (hyperfine) transition, in contrast, the hyperfine-induced M2 radiative channel is much weaker when compared to the leading E1 channel, and hence only the E1 decay is taken into account in this case.

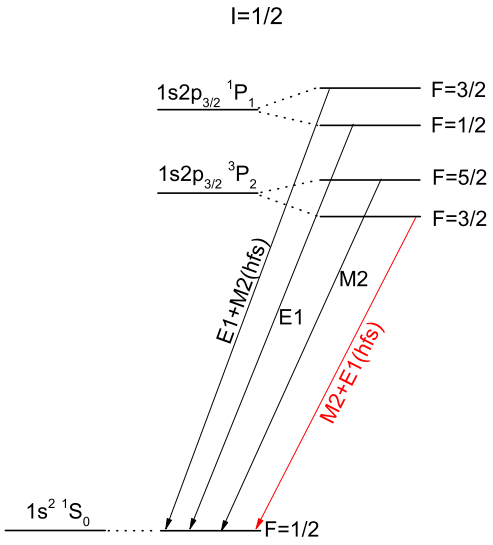

FIG. 1. (Color online) The fine- and hyperfine-level scheme for the $1s^2\ ^1S_0$ ground level and the $1s2p_{3/2}\ ^{1,3}P_{1,2}$ excited levels of heliumlike ions with nuclear spin $I = 1/2$.

Figure 1 displays the fine- and hyperfine-level scheme for the $1s^2\ ^1S_0$ ground state and the $1s2p_{3/2}\ ^{1,3}P_{1,2}$ excited levels of heliumlike ions with nuclear spin $I = 1/2$. Apart from the $F = 3/2$ levels, only one multipole transition occurs in their decay to the ground state and, hence, their structure function simply becomes a "geometrical" constant, independent of the particular amplitude [20,21]. In Eq. (9), therefore, only the two amplitudes $a_{\rm E1}$ and $a_{\rm M2}$ occur explicitly. For heliumlike ions (isotopes) with zero nuclear spin $I = 0$, in contrast, there is no hyperfine level splitting and, thus, the effective anisotropy parameter follows directly from averaging over the two fine-structure components [21],

$$\beta_2^{\rm eff}(K\alpha_1; I = 0) = \frac{1}{\sqrt{2}} N_{J=1} \mathcal{A}_{20}(^1P_1) - \sqrt{\frac{5}{14}} N_{J=2} \mathcal{A}_{20}(^3P_2), \tag{10}$$

which purely depends on the weight factors and the alignment parameters of the excited $1s2p_{3/2}\ ^{1,3}P_{1,2}$ levels, independent of any nuclear parameters or the amplitudes of the associated transitions.

C. Evaluation of transition amplitudes

As seen from Eq. (9), the computation of the *effective* anisotropy parameter $\beta_2^{\rm eff}(K\alpha_1, I = 1/2)$ for ions with nuclear spin $I = 1/2$ can be traced back to the reduced radiative amplitudes $\langle \beta_f F_f \| H_\gamma(pL) \| \beta_i F_i \rangle$ of the corresponding hyperfine transitions. In order to compute these reduced matrix elements,

one has to solve the secular equation:

$$(\hat{H}_0 + \hat{H}_{\rm hfs})|\beta F M_F\rangle = E_{\beta F}|\beta F M_F\rangle, \tag{11}$$

where $|\beta F M_F\rangle$ denotes the hyperfine wave function with the corresponding energy eigenvalue $E_{\beta F}$, and where $\hat{H}_0$ and $\hat{H}_{\rm hfs}$ represent the electronic Hamiltonian as well as the hyperfine-interaction Hamiltonian, respectively. The latter can be written as

$$\hat{H}_{\rm hfs} = \sum_{k\geqslant 1} T^{(k)} \cdot M^{(k)}, \tag{12}$$

with $T^{(k)}$ and $M^{(k)}$ being the k-order spherical tensor operators of the electronic and nuclear parts. If, as in the following, we only consider the dominant magnetic dipole interaction, we have

$$\hat{H}_{\rm hfs} = T^{(1)} \cdot M^{(1)}. \tag{13}$$

Assuming that we have already solved Eq. (11) for $\hat{H}_0$, i.e., the atomic (fine-structure) levels, the hyperfine-resolved states can be written as a linear combination of basis states that are constructed from products of the atomic states $|\alpha J M_J\rangle$ *times* the basis states for the nucleus, $|I M_I\rangle$:

$$\begin{aligned}|\beta F M_F\rangle &= \sum_{\alpha J} C^F_{\alpha J}|\alpha J I : F M_F\rangle \\ &\equiv \sum_{\alpha J}\sum_{M_I M_J} C^F_{\alpha J}\langle I M_I J M_J|F M_F\rangle|I M_I\rangle|\alpha J M_J\rangle.\end{aligned} \tag{14}$$

By inserting this ansatz into Eq. (11) and projecting it upon some basis state, we find that the (hyperfine) mixing coefficients $C^F_{\alpha J}$ satisfy the eigenvalue equation

$$E_{\beta F} C^F_{\alpha J} = \sum_{\alpha' J'} \left(E_{\alpha J}\delta_{\alpha\alpha'}\delta_{J J'} + W^F_{\alpha J,\alpha' J'}\right) C^F_{\alpha' J'}, \tag{15}$$

where $E_{\alpha J}$ is the energy eigenvalue of the corresponding fine-structure level $|\alpha J\rangle$, and where the interaction matrix elements

$$\begin{aligned}W^F_{\alpha J,\alpha' J'} = (-1)^{I+J+F} &\begin{Bmatrix} I & J & F \\ J' & I & 1 \end{Bmatrix} \\ &\times \langle \alpha J\|T^{(1)}\|\alpha' J'\rangle\langle I\|M^{(1)}\|I\rangle\end{aligned} \tag{16}$$

are given in terms of the reduced electronic and nuclear matrix elements, respectively. While a proper representation of the atomic state vectors is needed in order to evaluate the electronic amplitudes [25,26], the reduced nuclear amplitudes are simply obtained from

$$\langle I\|M^{(1)}\|I\rangle = \mu_I\sqrt{(2I+1)(I+1)/I}, \tag{17}$$

in terms of the magnetic dipole moment μ_I of the particular isotope under consideration.

As seen from Eqs. (16) and (17), the nuclear magnetic moment μ_I enters into the mixing coefficients $C^F_{\alpha J}$ and, hence, into the reduced (radiative) amplitudes [20],

$$\begin{aligned}\langle \beta_f F_f\|\, H_\gamma(pL)\,\|\beta_i F_i\rangle = &\sum_{\alpha_i J_i}\sum_{\alpha_f J_f} C^{F_i}_{\alpha_i J_i}\, C^{F_f}_{\alpha_f J_f}[F_i,F_f]^{1/2} \\ &\times (-1)^{J_i+I+F_f+L}\begin{Bmatrix} F_i & F_f & L \\ J_f & J_i & I \end{Bmatrix} \\ &\times \langle \alpha_f J_f\|\, H_\gamma(pL)\,\|\alpha_i J_i\rangle.\end{aligned} \tag{18}$$

In order to calculate these amplitudes for the hyperfine-resolved transitions of interest, we use the multiconfiguration Dirac-Fock (MCDF) method, in particular, the GRASP92 code [27] for generating the ionic wave functions and the RATIP program [26] for calculating all of the required REC cross sections, alignment parameters, hyperfine mixing coefficients, as well as radiative transition amplitudes.

III. RESULTS AND DISCUSSIONS

We are now prepared to make use of Eqs. (5)–(8) and to analyze the angular properties of the characteristic $K\alpha_1$ line following the REC into the excited $1s2p_{3/2}\ ^{1,3}P_{1,2}$ levels of heliumlike ions. For isotopes with $I \geqslant 1/2$, especially, the $K\alpha_1$ angular emission of heliumlike ions appears to be rather different when compared to isotopes of the same element but with *zero* nuclear spin, $I = 0$. Apart from the fine and hyperfine structures of the ions themselves, of course, the $K\alpha_1$ angular emission depends first of all also on the details of the excitation process. We shall consider here the radiative decay of the (heliumlike) ions following the REC into initially hydrogenlike projectiles with energies of about $T_p = 10$–200 MeV/u. Such energies are quite typical for the collision of high-Z projectiles with some gas target and have been explored before, for example, at ion storage rings. For these projectile energies, moreover, the alignment parameters A_{20} have been calculated at several places [14,21]. Below, we shall analyze and discuss in detail the effects of the hyperfine interaction upon the angular properties of the overall $K\alpha_1$ emission.

A. Ions with nuclear spin $I = 1/2$

For heliumlike ions in the excited $1s2p_{3/2}\ ^{1,3}P_{1,2}$ levels and for a nonzero alignment, a more or less strong anisotropy is usually found and is well known for the associated $K\alpha_1$ x-ray emission. Here, however, we are mainly interested in the modifications to the overall $K\alpha_1$ emission for isotopes with nonzero nuclear spin and magnetic moment owing to their hyperfine interaction. For example, Fig. 2 displays the effective anisotropy parameter $\beta_2^{\rm eff}$ of the total $K\alpha_1$ emission as functions of nuclear magnetic dipole moment μ_I, following the REC into initially hydrogenlike ions. In this figure, all calculations were performed for a projectile energy $T_p = 50$ MeV/u. Results are shown for isotopes with zero nuclear spin $I = 0$ (shadowed area) as well as for selected tin isotopes $^{A}_{50}\mathrm{Sn}^{48+}$ ($A = 119, 113, 121$; black points), xenon isotopes $^{A}_{54}\mathrm{Xe}^{52+}$ ($A = 129, 127, 125, 123$; red squares), and thallium isotopes $^{A}_{81}\mathrm{Tl}^{79+}$ ($A = 187, 205, 207$; blue triangles) [28], all with nuclear spin $I = 1/2$. While, for zero nuclear spin, the effective anisotropy parameter $\beta_2^{\rm eff}(K\alpha_1;\ I = 0)$ is nearly the same for all given medium- and high-Z elements, the parameters $\beta_2^{\rm eff}(K\alpha_1; I = 1/2)$ decrease roughly linear with

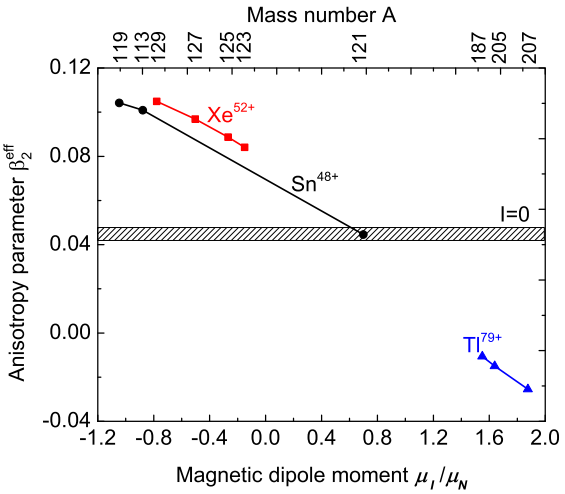

FIG. 2. (Color online) Effective anisotropy parameter $\beta_2^{\rm eff}$ of the $K\alpha_1$ characteristic emission as functions of the magnetic dipole moment μ_I following the REC into the two excited $1s2p_{3/2}\ ^{1,3}P_{1,2}$ levels of (finally) heliumlike projectiles with kinetic energy $T_p = 50$ MeV/u. Results are shown for the ${}^{A}_{50}\mathrm{Sn}^{48+}$ ($A = 119, 113, 121$; black points), ${}^{A}_{54}\mathrm{Xe}^{52+}$ ($A = 129, 127, 125, 123$; red squares), and ${}^{A}_{81}\mathrm{Tl}^{79+}$ ($A = 187, 205, 207$; blue triangles) isotopes as well as their zero-spin counterparts (shadowed area), respectively. Lines are drawn as a guide to the eyes.

the nuclear magnetic moment of the isotopes. The sign and particular values of the $\beta_2^{\rm eff}$ parameter hereby depend on the alignment parameters of the fine-structure levels as well as the admixture of the hyperfine-induced E1 to the leading M2 amplitudes in the hyperfine-resolved $1s2p_{3/2}\ ^3P_2$, $F_i = 3/2 \rightarrow 1s^2\ ^1S_0$, $F_f = 1/2$ transition.

If, for example, we consider the tin isotope ${}^{119}_{50}\mathrm{Sn}^{48+}$ with the negative magnetic moment $\mu_I = -1.047\,\mu_N$, the effective anisotropy $\beta_2^{\rm eff}(K\alpha_1)$ increases from 0.04 to 0.104, when compared to other tin isotopes with zero spin. Such a quite sizable change in the effective anisotropy parameter $\beta_2^{\rm eff}$ can be easily measured by using present-day detection techniques [4,13]. For thallium, moreover, all nuclear spin-1/2 isotopes have a rather large positive magnetic moment, as shown in Ref. [28], which gives rise to a negative effective anisotropy $\beta_2^{\rm eff}(K\alpha_1)$. An analog increase or decrease in the effective anisotropy parameter will also occur for other spin-1/2 isotopes in dependence of the particular sign and magnitude of their magnetic dipole moment μ_I.

Until now, we have discussed only the effective anisotropy parameter $\beta_2^{\rm eff}$ for just the energy $T_p = 50$ MeV/u of the projectile ions when colliding with electrons of an atomic gas target. For other projectile energies, of course, this parameter will vary owing to the changes in the initial alignment of the excited states. In order to better understand the associated modifications in the $K\alpha_1$ anisotropy, Fig. 3 displays the effective anisotropy parameter $\beta_2^{\rm eff}(K\alpha_1)$ as functions of the projectile energy T_p. Results are shown for the tin isotope ${}^{119}_{50}\mathrm{Sn}^{48+}$ with $I = 1/2$ and $\mu_I = -1.047\,\mu_N$ (left panel), as well as for the thallium isotope ${}^{207}_{81}\mathrm{Tl}^{79+}$ with $I = 1/2$ and $\mu_I = +1.876\,\mu_N$ (right panel), respectively. Again, detailed computations for these two spin-1/2 isotopes (black solid lines), and with magnetic moments of different sign, are

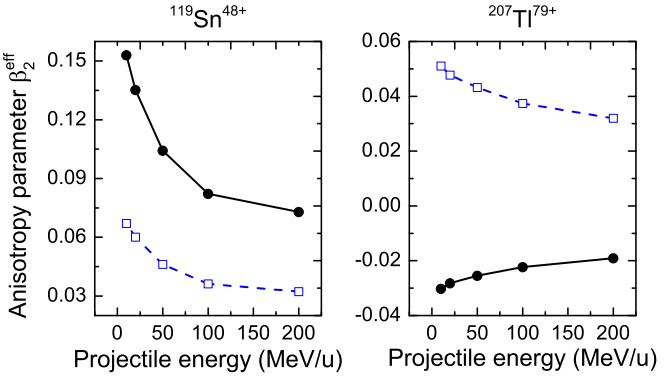

FIG. 3. (Color online) Effective anisotropy parameter $\beta_2^{\rm eff}$ of the $K\alpha_1$ characteristic emission as functions of the projectile energy T_p following the REC into the two excited $1s2p_{3/2}\ ^{1,3}P_{1,2}$ levels of (finally) heliumlike ions. Results are shown for the ${}^{119}_{50}\mathrm{Sn}^{48+}$ ($I = 1/2$, $\mu_I = -1.047\,\mu_N$; left panel) and ${}^{207}_{81}\mathrm{Tl}^{79+}$ ($I = 1/2$, $\mu_I = +1.876\,\mu_N$; right panel) isotopes, respectively. Computations for the two spin-1/2 isotopes (black solid lines) are compared with those for zero-spin isotopes of the same elements (blue dashed lines).

compared with those for zero-spin isotopes of the same elements (blue dashed lines). As clearly seen from this figure, a significant but different shift in the anisotropy parameter is observed in these two cases. While for the thallium isotope ${}^{207}_{81}\mathrm{Tl}^{79+}$, for example, the effective anisotropy parameter is always negative at all projectile energies due to its large and positive magnetic moment $\mu_I = +1.876\,\mu_N$, the biggest effect of the hyperfine interaction is usually observed for low projectile energies at which the REC gives rise to the strongest alignment of the excited $1s2p_{3/2}\ ^{1,3}P_{1,2}$ levels and, hence, to a large effective anisotropy parameter $\beta_2^{\rm eff}(K\alpha_1)$.

The quite large difference in the effective anisotropy parameter $\beta_2^{\rm eff}(K\alpha_1)$ for zero-spin and spin-1/2 isotopes of the same element makes the measurement of the angular distribution a sensitive tool for determining the nuclear spin and magnetic moment, i.e., nuclear parameters, via their influence upon the overall $K\alpha_1$ emission. Figure 4, for

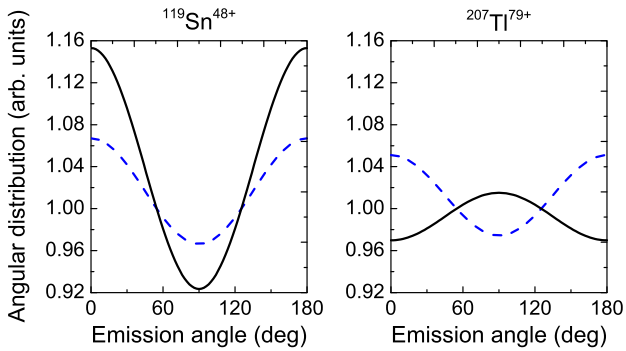

FIG. 4. (Color online) Angular distribution of the $K\alpha_1$ characteristic emission following the REC into the excited $1s2p_{3/2}\ ^{1,3}P_{1,2}$ levels of (finally) heliumlike ions. Results for the spin-1/2 isotopes from Fig. 3 (black solid lines) are compared with computations for zero-spin isotopes (blue dashed lines) of the same element. All calculations were performed within the projectile frame and for projectile ions with kinetic energy $T_p = 10$ MeV/u.

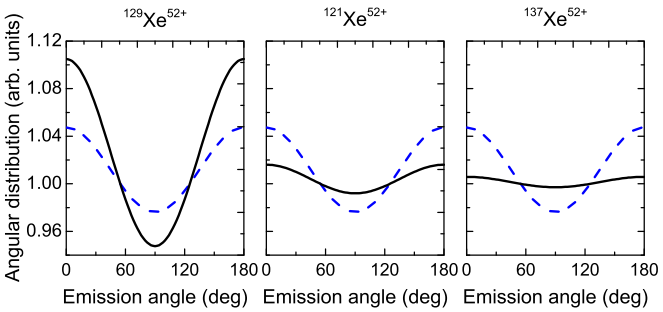

FIG. 5. (Color online) The same as Fig. 4, but for the projectile energy $T_p = 50$ MeV/u and for three different xenon isotopes with nuclear spin $I \geqslant 1/2$ and comparable magnetic dipole moment μ_I: $^{129}_{54}Xe^{52+}$ ($I = 1/2$, $\mu_I = -0.778\mu_N$; left panel), $^{121}_{54}Xe^{52+}$ ($I = 5/2$, $\mu_I = -0.701\mu_N$; middle panel), and $^{137}_{54}Xe^{52+}$ ($I = 7/2$, $\mu_I = -0.968\mu_N$; right panel).

example, shows the corresponding angular distribution for the two isotopes $^{119}_{50}Sn^{48+}$ and $^{207}_{81}Tl^{79+}$ from Fig. 3 and for the quite small projectile energy, $T_p = 10$ MeV/u. Once again, results for these two spin-1/2 isotopes with opposite sign of the magnetic moment (black solid lines) are compared with those for their zero-spin counterparts (blue dashed lines). Of course, the (remarkable) change in the angular distribution of the $K\alpha_1$ emission from the heliumlike thallium (right panel) results again from the change in the sign of the anisotropy parameter, as discussed above. Note that this is a case in the physics of medium- and high-Z ions in which the hyperfine interaction results in a qualitatively different (angular) behavior of the emitted x-ray emission, compared to what one expects for the corresponding zero-spin isotopes with natural abundance.

B. Ions with nuclear spin $I > 1/2$

Apart from the spin-zero data, all computations performed above refer to spin-1/2 isotopes, in which just a hyperfine doublet occurs for each fine-structure level with $J \neq 0$. For the $K\alpha_1$ decay of the upper $1s2p_{3/2}\ ^3P_2$ level, especially, the hyperfine coupling between the $1s2p_{3/2}\ ^3P_2$ and $^1P_1$ levels then induces the E1 admixture to the $1s2p_{3/2}\ ^3P_2 \rightarrow 1s^2\ ^1S_0$ fine-structure transition that significantly affects the M2 emission pattern of this fine-structure transition. A similar E1-M2 multipole mixing also occurs for other isotopes with nuclear spin $I > 1/2$, but with less influence upon the overall $K\alpha_1$ emission owing to the reduced weight of this (single) hyperfine transition. More generally, each fine-structure level splits into $|J - I|, |J - I| + 1, \ldots, J + I$ hyperfine levels from which only either two or three (hyperfine) transitions may benefit from a significant E1 admixture. Therefore, the effect of the hyperfine interaction will be lowered as the nuclear spin increases. This can be seen also from Fig. 5, which compares the angular distribution of the $K\alpha_1$ line for different xenon isotopes with nuclear spin $I = 1/2$, $5/2$, and $7/2$, respectively. To facilitate the comparison, we have chosen here three isotopes with a comparable (negative) magnetic moment.

IV. CONCLUSION

In summary, we have explored the angular distribution of the $K\alpha_1$ emission following the REC into the excited $1s2p_{3/2}\ ^{1,3}P_{1,2}$ levels of (finally) heliumlike ions with nonzero nuclear spin, $I \neq 0$. Special attention has been given to the effect of the hyperfine interaction and how the hyperfine splitting of fine-structure transitions of heliumlike ions affects the overall $K\alpha_1$ x-ray emission. Detailed computations within the density matrix theory and the multiconfiguration Dirac-Fock method were performed for selected isotopes of heliumlike Sn^{48+}, Xe^{52+}, and Tl^{79+} ions. These computations showed that the hyperfine interaction may quite significantly influence the $K\alpha_1$ angular properties for realistic values of the magnetic (dipole) moments μ_I and especially for nuclear spin $I = 1/2$, while this effect becomes weaker as the nuclear spin increases.

From this theoretical analysis, we suggest that accurate measurements of the $K\alpha_1$ angular emission at ion storage rings can be utilized as an independent tool for determining the nuclear parameters of rare stable or radioactive isotopes with $I \geqslant 1/2$.

ACKNOWLEDGMENTS

ZWW thanks the Helmholtz Institute Jena and the Helmholtz Association for financial support. AS acknowledges the support from the Helmholtz Association under Project No. VH-NG-421.

[1] A. Surzhykov, S. Fritzsche, A. Gumberidze, and T. Stöhlker, Phys. Rev. Lett. **88**, 153001 (2002).
[2] S. Fritzsche, A. Surzhykov, and Th. Stöhlker, Phys. Rev. Lett. **103**, 113001 (2009).
[3] Th. Stöhlker, C. Kozhuharov, P. H. Mokler, A. Warczak, F. Bosch, H. Geissel, R. Moshammer, C. Scheidenberger, J. Eichler, A. Ichihara, T. Shirai, Z. Stachura, and P. Rymuza, Phys. Rev. A **51**, 2098 (1995).
[4] G. Weber, H. Bräuning, A. Surzhykov, C. Brandau, S. Fritzsche, S. Geyer, S. Hagmann, S. Hess, C. Kozhuharov, R. Märtin, N. Petridis, R. Reuschl, U. Spillmann, S. Trotsenko, D. F. A. Winters, and Th. Stöhlker, Phys. Rev. Lett. **105**, 243002 (2010).
[5] Z. M. Hu, X. Y. Han, Y. M. Li, D. Kato, X. M. Tong, and N. Nakamura, Phys. Rev. Lett. **108**, 073002 (2012).
[6] J. Eichler and W. Meyerhof, *Relativistic Atomic Collisions* (Academic, San Diego, 1995).
[7] G. A. Machicoane, T. Schenkel, T. R. Niedermayr, M. W. Newmann, A. V. Hamza, A. V. Barnes, J. W. McDonald, J. A. Tanis, and D. H. Schneider, Phys. Rev. A **65**, 042903 (2002).
[8] S. Fritzsche, A. Surzhykov, A. Gumberidze, and T. Stöhlker, New J. Phys. **14**, 083018 (2012).
[9] J. M. Bizau, J. M. Esteva, D. Cubaynes, F. J. Wuilleumier, C. Blancard, A. C. La Fontaine, C. Couillaud, J. Lachkar, R. Marmoret, C. Rémond, J. Bruneau, D. Hitz, P. Ludwig, and M. Delaunay, Phys. Rev. Lett. **84**, 435 (2000).
[10] S. Fritzsche, P. Indelicato, and Th. Stöhlker, J. Phys. B **38**, S707 (2005).

[11] M. S. Pindzola, Sh. A. Abdel-Naby, F. Robicheaux, and J. Colgan, Phys. Rev. A **85**, 032701 (2012).
[12] Th. Stöhlker, F. Bosch, A. Gallus, C. Kozhuharov, G. Menzel, P. H. Mokler, H. T. Prinz, J. Eichler, A. Ichihara, T. Shirai, R. W. Dunford, T. Ludziejewski, P. Rymuza, Z. Stachura, P. Swiat, and A. Warczak, Phys. Rev. Lett. **79**, 3270 (1997).
[13] X. Ma, P. H. Mokler, F. Bosch, A. Gumberidze, C. Kozhuharov, D. Liesen, D. Sierpowski, Z. Stachura, T. Stöhlker, and A. Warczak, Phys. Rev. A **68**, 042712 (2003).
[14] A. Surzhykov, U. D. Jentschura, Th. Stöhlker, and S. Fritzsche, Phys. Rev. A **74**, 052710 (2006).
[15] A. Surzhykov, U. D. Jentschura, Th. Stöhlker, and S. Fritzsche, Eur. Phys. J. D **46**, 27 (2008).
[16] S. Tashenov, Th. Stöhlker, D. Banaś, K. Beckert, P. Beller, H. F. Beyer, F. Bosch, S. Fritzsche, A. Gumberidze, S. Hagmann, C. Kozhuharov, T. Krings, D. Liesen, F. Nolden, D. Protic, D. Sierpowski, U. Spillmann, M. Steck, and A. Surzhykov, Phys. Rev. Lett. **97**, 223202 (2006).
[17] J. R. Henderson, P. Beiersdorfer, C. L. Bennett, S. Chantrenne, D. A. Knapp, R. E. Marrs, M. B. Schneider, K. L. Wong, G. A. Doschek, J. F. Seely, C. M. Brown, R. E. LaVilla, J. Dubau, and M. A. Levine, Phys. Rev. Lett. **65**, 705 (1990).
[18] J. Dubau, Y. Garbuzov, and A. Urnov, Phys. Scr. **49**, 39 (1994).
[19] R. Bensaid, M. K. Inal, and J. Dubau, J. Phys. B **39**, 4131 (2006).
[20] A. Surzhykov, Y. Litvinov, Th. Stöhlker, and S. Fritzsche, Phys. Rev. A **87**, 052507 (2013).
[21] A. Surzhykov, U. D. Jentschura, Th. Stöhlker, and S. Fritzsche, Phys. Rev. A **73**, 032716 (2006).
[22] K. Blum, *Density Matrix Theory and Applications* (Plenum, New York, 1981).
[23] V. V. Balashov, A. N. Grum-Grzhimailo, and N. M. Kabachnik, *Polarization and Correlation Phenomena in Atomic Collisions* (Kluwer Academic, New York, 2000).
[24] In this formula, we assume here that the hyperfine interaction does not affect the excitation, i.e., the first step of process (1).
[25] W. R. Johnson, Can. J. Phys. **89**, 429 (2011).
[26] S. Fritzsche, Comput. Phys. Commun. **183**, 1525 (2012).
[27] F. A. Parpia, C. F. Fischer, and I. P. Grant, Comput. Phys. Commun. **94**, 249 (1996).
[28] N. J. Stone, At. Data Nucl. Data Tables **90**, 75 (2005).